AIP | The Journal of Chemical Physics

Nucleation of liquid droplets and voids in a stretched Lennard-Jones fcc crystal

Vladimir G. Baidakov and Azat O. Tipeev

Citation: The Journal of Chemical Physics **143**, 124501 (2015); doi: 10.1063/1.4931108
View online: http://dx.doi.org/10.1063/1.4931108
View Table of Contents: http://scitation.aip.org/content/aip/journal/jcp/143/12?ver=pdfcov
Published by the AIP Publishing

Articles you may be interested in

Crystallization of Lennard-Jones nanodroplets: From near melting to deeply supercooled
J. Chem. Phys. **142**, 124506 (2015); 10.1063/1.4915917

Surface induced nucleation of a Lennard-Jones system on an implicit surface at sub-freezing temperatures: A comparison with the classical nucleation theory
J. Chem. Phys. **139**, 234707 (2013); 10.1063/1.4848737

The physics of nucleated droplets in large-scale MD Lennard-Jones simulations
AIP Conf. Proc. **1527**, 23 (2013); 10.1063/1.4803195

Cavitation and crystallization in a metastable Lennard-Jones liquid at negative pressures and low temperatures
J. Chem. Phys. **135**, 054512 (2011); 10.1063/1.3623587

Crystal nucleation rate isotherms in Lennard-Jones liquids
J. Chem. Phys. **132**, 234505 (2010); 10.1063/1.3439585

This article is copyrighted as indicated in the article. Reuse of AIP content is subject to the terms at: http://scitation.aip.org/termsconditions. Downloaded to IP: 35.8.11.3 On: Fri, 29 Jan 2016 23:26:19

Nucleation of liquid droplets and voids in a stretched Lennard-Jones fcc crystal

Vladimir G. Baidakov[a] and Azat O. Tipeev
Institute of Thermophysics, Ural Branch of the Russian Academy of Sciences, Amundsen Street 107a, 620016 Ekaterinburg, Russia

(Received 29 June 2015; accepted 3 September 2015; published online 22 September 2015)

The method of molecular dynamics simulation has been used to investigate the phase decay of a metastable Lennard-Jones face-centered cubic crystal at positive and negative pressures. It is shown that at high degrees of metastability, crystal decay proceeds through the spontaneous formation and growth of new-phase nuclei. It has been found that there exists a certain boundary temperature. Below this temperature, the crystal phase disintegrates as the result of formation of voids, and above, as a result of formation of liquid droplets. The boundary temperature corresponds to the temperature of cessation of a crystal–liquid phase equilibrium when the melting line comes in contact with the spinodal of the stretched liquid. The results of the simulations are interpreted in the framework of classical nucleation theory. The thermodynamics of phase transitions in solids has been examined with allowance for the elastic energy of stresses arising owing to the difference in the densities of the initial and the forming phases. As a result of the action of elastic forces, at negative pressures, the boundary of the limiting superheating (stretching) of a crystal approaches the spinodal, on which the isothermal bulk modulus of dilatation becomes equal to zero. At the boundary of the limiting superheating (stretching), the shape of liquid droplets and voids is close to the spherical one. © *2015 AIP Publishing LLC.* [http://dx.doi.org/10.1063/1.4931108]

I. INTRODUCTION

Solids usually melt from their surface. This is caused by the fact that the liquid phase wets, as a rule, the whole surface of the solid phase of the same substance. At these conditions, the appearance of a liquid layer on a solid does not require any work for the formation of a new surface, and, therefore, the superheating of a solid with an open surface is impossible.[1]

In contrast, a fluctuation-induced nucleation of a new phase in the bulk of a crystal may be observed at appropriate heating conditions, i.e., if the crystal is heated from the inside and the temperature of the surface is maintained lower than that of equilibrium melting,[2] or if heating is realized in time scales much shorter than the time required to melt the sample from the surface.[3,4] Another possibility of realizing a high degree of metastability in solids is connected with shock-wave experiments[5] and laser ablation.[6,7] When a shock wave is reflected from the free surface of a solid, tensile stresses are created in it, which may cause the appearance of voids.

The question of the maximum possible superheating (stretching) of a crystal is actively discussed in the literature. There are several well-known approaches to this problem. A number of approaches are based on mechanical and thermodynamic criteria. Thus, the Born model of shear instability determines the boundary of existence of the crystalline state by conditions leading to a vanishing of the shear modulus.[8] The Lindemann criterion predicts melting when the average amplitude of atomic oscillations in the lattice reaches its critical value.[9] Several versions of the so-called thermodynamic catastrophe theory have been suggested.[10,11] Reference 10 introduces the notion of an entropic catastrophe defining the temperature of the stability limit as the temperature at which the entropy of a superheated crystal becomes equal to that of the glassy phase. Tallon[11] modified this criterion by introducing a new point of stability loss, at which the specific volume of a crystal is equal to that of a liquid.

A different approach to the determination of the limiting superheating (stretching) of the crystalline state is connected with kinetic criteria and based on an analysis of the kinetics of homogeneous nucleation of a new phase in a metastable crystal.[12] In this case, the temperature of the limiting superheating is defined as the temperature corresponding to a certain rate of nucleation of a new phase.

New possibilities in studying spontaneous nucleation in superheated and stretched solids are opened up by the method of molecular dynamics (MD) simulation, which makes it possible to trace on the atomic level the process of nucleation and growth of new-phase inclusions and to determine thermodynamic and kinetic parameters of this process.[13–19] The absence of free boundary surfaces and defects of the crystal lattice in the model ensures the homogeneous mechanism of nucleation, and the short characteristic times of evolution of molecular dynamics models allow realizing superheatings and stretches close to the ideal strength of a crystal.

Lu and Li[13] determined the temperature at which one can observe an intensive formation of melt nuclei in a superheated Lennard-Jones (LJ) crystal by the value of $T_n \approx 1.2T_m$, where T_m is the melting temperature. According to data of Luo *et al.*[16] for different elements and simple compounds, the value of

[a]Author to whom correspondence should be addressed. Electronic mail: baidakov@itp.uran.ru

 © 2015 AIP Publishing LLC

This article is copyrighted as indicated in the article. Reuse of AIP content is subject to the terms at: http://scitation.aip.org/termsconditions. Downloaded to IP: 35.8.11.3 On: Fri, 29 Jan 2016 23:26:19

T_n varies within the limits (1.08–1.43)T_m with a rather weak dependence of T_n on the heating rate. The results of Refs. 13, 14, 16, and 18 refer to zero pressure. In a wide pressure range, including negative pressures, limiting superheatings of the crystal phase were investigated in Refs. 15, 17, and 19.

Along with the kinetic boundary of limiting superheating (stretching), Ref. 17 determined from the condition $(\partial p/\partial \rho)_T = 0$ the boundary of essential instability of the crystal phase, i.e., the spinodal. The values of tensile stresses that correspond to this boundary are known as "the ideal strength" of a crystal. At high temperatures, limiting stretching corresponding to the kinetic boundary and the spinodal differs considerably, and at $T \le 0.7T_m$, in the region of negative pressures, practically coincides.

Figure 1 presents the phase diagram of a simple one-component system. The lines of crystal–gas (sublimation line) and crystal–liquid (melting line) phase equilibrium have metastable extensions beyond the triple point. On the metastable extension of the sublimation line, the crystal and gas phases are in equilibrium, and they are metastable with respect to the liquid. On the melting line at $0 < p < p_t$, where p_t is the pressure at the triple point, the crystal and the liquid are metastable with respect to the gas phase. Metastable crystal–liquid equilibrium is also observed in the region of negative pressures, when the coexistent phases are under the action of stresses stretching in all directions. Metastable extensions of sublimation and melting lines end at the points of their contact, respectively, with the spinodal of a crystal K_1 and a stretched liquid K_2 (see Fig. 1).[17,20]

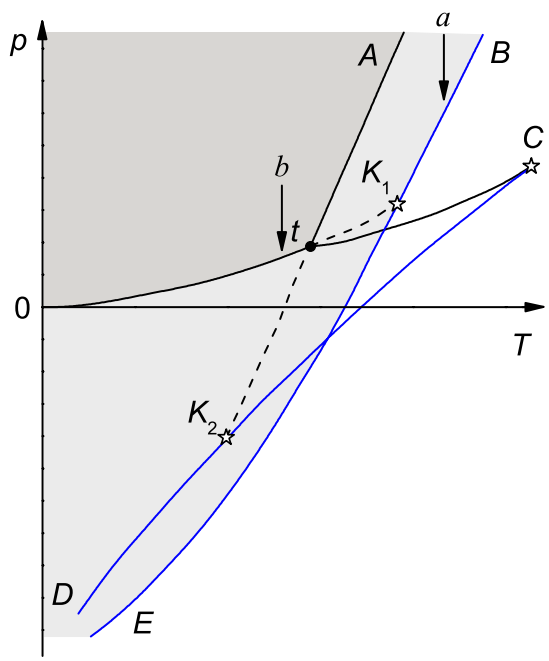

FIG. 1. Phase diagram of a simple one-component system in pressure p and temperature T coordinates. At and tK_2 are the melting line and its metastable extension, Ot and tK_1 the sublimation line and its metastable extension, tC is the line of liquid–gas phase equilibrium, CK_2D the spinodal of a stretched (superheated) liquid, BK_1E the spinodal of a stretched (superheated) crystal, t the triple point, C the liquid–gas critical point, K_1 the sublimation line endpoint, and K_2 the melting line endpoint. The dark gray area shows a stable crystalline state, the light gray area a region of a metastable crystal. For the arrows a, b, see the text.

At negative pressures, depending on the value of stretching, the melting of a crystal may proceed by the formation of a liquid-phase nucleus. Another way of removal of phase metastability here is the appearance of some discontinuity. The gas phase has no resistance to stretching and at $p < 0$ can exist in neither a stable nor a metastable state. The formation of potential centers of discontinuity, as well as of melting, may proceed by way of fluctuation nucleation of voids (holes). Which of the indicated processes, discontinuity or melting, at given thermodynamic parameters (p, T) will determine the rupture of a crystal phase is the topic of investigation of the present paper.

The paper examines thermodynamic and kinetic aspects of nucleation of a new phase in a stretched crystal. The analysis is performed based on the results of molecular dynamics simulations of the nucleation process in a Lennard-Jones crystal with a face-centered cubic (fcc) lattice. The formation of new-phase nuclei in the bulk of a stretched (superheated) solid is considered in Sec. II. The details of simulation and the procedure of calculating the basic parameters are given in Sec. III. Sec. IV presents the results of simulation and their discussion. Sec. V provides a summary of conclusions from the present investigations.

II. NUCLEATION IN SOLIDS

Let us consider the formation of a liquid phase (phase l) in an unbounded isotropic solid elastic medium (phase s), which is under the action of an external hydrostatic pressure p and has a temperature T. The phase l is characterized by the bulk modulus K_l. The shear modulus μ_s and the bulk modulus K_s have been introduced for describing the elastic properties of the phase s. If in the process of a phase transition no relaxation of internal stresses is observed, the change in the Gibbs free energy G connected with the appearance of new-phase inclusions may be presented as follows:[21,22]

$$\Delta G = (\Delta g + e)\, V + \gamma_{sl} A, \tag{1}$$

where $\Delta g(p) = g_l - g_s$ is the difference of the specific (referred to unit volume) thermodynamic potentials, γ_{sl} is the solid–liquid interfacial free energy, V is the volume of a new-phase inclusion, A is the area of its surface, e is the elastic energy density (per unit volume) resulting from the volume change upon melting

$$e = \frac{1}{2} K_{eff} \left(\frac{\Delta \upsilon}{\upsilon} \right)^2, \tag{2}$$

K_{eff} is the effective elastic modulus, and $\Delta\upsilon/\upsilon = (\upsilon_l - \upsilon_s)/\upsilon_l$ is the relative difference of the specific volumes of the liquid and the solid phases.

At given values of p and V, the value of e depends on the shape of the surface of the inclusion. This shape has to be determined from the minimum condition of the potential ΔG. If a liquid-phase inclusion has the shape of a sphere of radius R, then $V = 4\pi R^3/3$, $A = 4\pi R^2$, and

$$K_{eff} = \frac{4 K_l \mu_s}{3K_l + 4\mu_s}. \tag{3}$$

This article is copyrighted as indicated in the article. Reuse of AIP content is subject to the terms at: http://scitation.aip.org/termsconditions. Downloaded to IP: 35.8.11.3 On: Fri, 29 Jan 2016 23:26:19

The value of ΔG is numerically equal to the work of formation of a liquid droplet W in a metastable solid at fixed values of p and T. As a function of R, the Gibbs excess free energy has a finite maximum at

$$R_* = \frac{-2\gamma_{sl}}{\Delta g + e}. \tag{4}$$

The extreme value of $W = W_*$ corresponds to the formation of a nucleus which is in equilibrium with the medium

$$W_* = \frac{16\pi\gamma_{sl}^3}{3(\Delta g + e)^2}. \tag{5}$$

Equations (4) and (5) determine, respectively, the radius of a critical nucleus R_* and the work of its formation W_*.

At a small degree of metastability of a crystal phase, the value of Δg may be expressed in terms of the parameters of the phase-equilibrium line. In the case of isothermal stretching (T = const), we get

$$\Delta g = -(p_m - p)(\Delta\upsilon/\upsilon_l), \tag{6}$$

where p_m is the pressure on the melting line at temperature T.

If entry into the region of metastable state of a crystal is achieved by its isobaric heating (p = const), then

$$\Delta g = -(q/T_m)(T - T_m), \tag{7}$$

where T_m is the melting temperature, and q is the melting heat per unit volume at pressure p. For high superheatings, in Eq. (7), q denotes the value of the melting heat determined by the average values of the liquid and crystal entropies on the interval (T_m, T). Similarly, in Eq. (6), υ_s and υ_l are the average values of specific volumes on the interval (p_m, p).

According to Eq. (5), at given values of p and T, the work of formation of a critical nucleus in an elastic medium will exceed that in a fluid phase ($|\Delta g + e| < |\Delta g|$). The radius of a critical nucleus will be bigger too. If with the appearance of a new phase internal stresses do not arise (in Eq. (5) $e = 0$), then nucleation may begin right after the intersection of the phase equilibrium line. Here, at $\Delta g \to 0$, the critical size of a nucleus tends to infinity. If $e \neq 0$, the required condition of formation of a new phase is $\Delta g + e < 0$. Otherwise, the expenditure of energy for the creation of a field of internal stresses exceeds the energy gain from the formation of a thermodynamically more stable phase. The equation

$$\Delta g + e = 0 \tag{8}$$

corresponds in such case to the equilibrium of the phase s with a macroscopic amount of the phase l and determines the line of beginning of an $s \to l$ phase transition: at $(\Delta g + e) \to 0$, the critical size increases without limit. From Eq. (8) follows the existence of a region forbidden for phase transitions beyond the melting line, which is limited in temperature from above by the value of $-\Delta g_c = e$ and is known in the literature as the region of elastic thermodynamic hysteresis.[22]

Elastic forces, which arise owing to the difference in the densities of the different phases, make the formation of a spherical liquid-phase nucleus in the nearest vicinity of the melting line thermodynamically unprofitable. Moreover, a spherical shape of a nucleus is in the general case not the optimum form even in an isotropic medium. It can be shown[23,24] that at low superheatings of a solid phase a nucleus in the form of a highly flattened disk (lense) of radius R and height $h << R$ is more energy-efficient. In this case, $V = bR^2h$, $A = 2\pi R^2$, where b is a numerical coefficient dependent on the details of the shape of the nucleus. The effective elastic modulus for such a nucleus[23] is

$$K_{eff} = \frac{\pi\mu_s}{2(1 - \upsilon_s)}\frac{h}{R}, \tag{9}$$

where υ_s is the Poisson coefficient. As distinct from a spherical nucleus, the value of K_{eff} in Eq. (9) does not depend on the elastic characteristics of the liquid phase.

The work of formation of a lense-shaped nucleus, as a function of R and h, has the shape of a saddle. The dimensions of a critical nucleus are determined by the position of the saddle point,[24,25]

$$R_* = \frac{4\pi^2\gamma_{sl}\mu_s}{3b(1 - \upsilon_s)(\Delta g)^2}\left(\frac{\Delta\upsilon}{\upsilon}\right)^2, \tag{10}$$

$$h_* = \frac{-8\pi\gamma_{sl}}{3b\,\Delta g}. \tag{11}$$

The work of formation of a critical nucleus in this case takes the form

$$W_* = \frac{2\pi^3\gamma_{sl}^3\mu_s^2}{3(1 - \upsilon_s)^2(\Delta g)^4}\left(\frac{\Delta\upsilon}{\upsilon}\right)^4. \tag{12}$$

As distinct from Eqs. (10) and (11), Eq. (12) does not contain the factor b. With the requirement for Eq. (12) to coincide with the well-known Gibbs formula $W_* = \gamma_{sl}A_*/3$, taking into account Eq. (10), we have $b = 4\pi/3$.

From Eqs. (10)–(12), it follows that at small values of Δg as it is wished, the critical nucleus does exist, and, consequently, there is no elastic thermodynamic hysteresis. However, the elastic forces lead to a considerable difference in the work of formation of a critical nucleus ($W_* \sim (\Delta g)^{-4}$) in a solid from the work in a fluid phase, where $W_* \sim (\Delta g)^{-2}$. According to Eqs. (10) and (11), $h_*/R_* \sim \Delta\mu$, i.e., low superheatings are characterized by critical nuclei highly flattened in one dimension. At high superheatings, the second term in the brackets of Eq. (1) is small as compared with the first one. At a prescribed volume of a critical nucleus, its shape will be determined from the condition of minimum of the surface energy. This will lead to the sphericalization of a nucleus. Thus, at $|\Delta g| > |\Delta g_c|$, a transition from lense-shaped to spherical critical nuclei is possible.

Expression (1) for ΔG has been obtained under the assumption that the deformations have a purely elastic character. If the volume jump in a phase transition is large enough, and there is a considerable difference in the bulk moduli of the liquid and solid phases, a zone of plastic deformation may form in the solids. The presence of a plastic interlayer leads to a decrease in e as compared with the case of an ideal elastic medium, and will thereby contribute to the appearance of spherical nuclei.[25]

At negative pressures, the decay of a metastable crystal may proceed not only through the formation of liquid-phase nuclei but also by fluctuation-induced violation of continuity with the formation of voids (cavities) that do not contain a gas phase. In the latter case, for determining the characteristic sizes

This article is copyrighted as indicated in the article. Reuse of AIP content is subject to the terms at: http://scitation.aip.org/termsconditions. Downloaded to IP: 35.8.11.3 On: Fri, 29 Jan 2016 23:26:19

and the work of formation of a viable void, one can use the energy approach of Griffith.[26]

An isotropic elastic solid under the action of a constant stretching hydrostatic pressure $-p$ possesses a certain amount of elastic energy E. Let us designate as ΔE the change of this energy as a result of the appearance in the solid of a single void with a free surface of area A. Assuming that the released elastic energy is utilized for the formation of an interface, we can write

$$W = -\Delta E + \gamma_{sv} A, \tag{13}$$

where γ_{sv} is the crystal–gas interfacial free energy.

The value of ΔE depends on the shape of the void formed. In the case of a lense-shaped void, using the strict result of Sneddon[27] in the theory of cracks, for the radius R_*, volume V_*, and work of formation W_* of a critical nucleus, we have[26,27]

$$R_* = \frac{\pi \gamma_{sv} \mu_s}{(1-\upsilon_s) p^2}, \tag{14}$$

$$V_* = \frac{-4(1-\upsilon_s) p R_*^3}{3\mu_s}, \tag{15}$$

$$W_* = \frac{2\pi^3 \gamma_{sv}^3 \mu_s^2}{3(1-\upsilon_s)^2 p^4}. \tag{16}$$

The form of Eqs. (14) and (16) is similar to that of Eqs. (10) and (12). Since the specific volume of a gas phase is much larger than that of a crystal phase, and the sublimation pressure p_{sub} is close to zero, $\Delta\upsilon/\upsilon \approx 1$, and $\Delta g \approx -(p_{sub} - p) \approx p$. At the same time, there is a fundamental difference in the values of γ_{sl} and γ_{sv}, which will be discussed further.

III. SIMULATION DETAILS

A. Model

MD simulation has been performed in an ideal fcc crystal initially free of defects and open surfaces, in which the interaction between particles is described by the LJ potential. The potential was cut off at a distance $r_c = 6.58\sigma$ from the interaction center. The potential parameters σ and ε, which determine, respectively, the characteristic scales of length and energy, along with the Boltzmann constant k_B and the mass of a particle m, were used as the parameters of reduction of the quantities being calculated: temperature T in units ε/k_B, pressure p in units ε/σ^3, density in units σ^{-3}, and time in units $(m\sigma^2/\varepsilon)^{1/2}$. Further, all the reduced quantities are designated by the superscript (*).

The systems under investigation contained $N = 32\,000$, 108 000, and 500 000 particles, which were located in a cubic cell with three-dimensional periodic boundary conditions. Calculations of the crystal properties were made at a constant temperature and volume (*NVT* ensemble). The process of nucleation and growth of a new phase in a crystal took place in conditions of constant energy and volume (*NVE* ensemble). The time step in the integration of the equations was 0.0023 in reduced unit. MD simulation was carried out with the use of parallel calculations in the LAMMPS program.[28]

B. Calculation of thermodynamic and mechanical properties

Homogeneous nucleation in a stretched LJ crystal was investigated at reduced temperatures $T^* = 0.4$, 0.55, 0.7, and 0.85. At $r_c{}^* = 6.58$, the temperature of the triple point $T_t{}^*$ is 0.692, and that of the endpoint of the melting line $T_{K2}{}^*$ is 0.529.[17] Calculations began in the stable region of a crystal. The particles were located at the sites of an ideal fcc lattice. For every temperature, with the exception of $T^* = 0.85$, the initial density was chosen in such a way that the reduced pressure was about 0.5. The crystal was stretched by a proportional increase in the cell sides. In the process of transition into a new state, the crystal temperature was maintained constant by a Berendsen thermostat.[29] After 10^5 time steps, when the relaxation processes in the system caused by the change of its thermodynamic state were completed, a calculation of thermodynamic (pressure and internal energy), mechanical (elastic constants), and structural (parameter of central symmetry (CSP)) crystal properties was carried out.

The results of calculating pressure as a function of density for the temperatures under investigation are presented in Fig. 2. Ibidem one can find the $p\rho T$–data for a LJ crystal from Ref. 30 the crystal branch of the melting line and its metastable extension (the dashed line), and also the crystal spinodal (by data of Ref. 17). The solid lines passing through the points show the results of calculating pressure by a thermal equation of state for a LJ crystal.[20]

The bulk modulus $K_s = -V(\partial p/\partial V)_T$ was calculated by differentiation of the dependence $p(\rho)$. In a cubic crystal, deformations without changes in the volume are characterized by the moduli c_{44} (in Voigt notation) and $\tilde{c}_{44} = (c_{11} - c_{12})/2$. The elastic constants c_{ij} were calculated as[31,32]

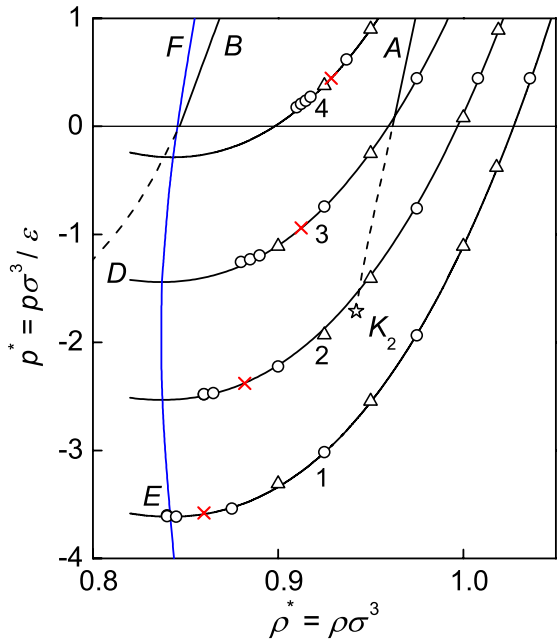

FIG. 2. Isotherms of a LJ crystal: 1 - $T^* = 0.4$, 2 - 0.55, 3 - 0.7, 4 - 0.85. ○ — data of the present work, △ — results of Ref. 30, the lines passing through points — by the equation of state of Ref. 20. *BD* and AK_2 are the liquid and crystal branches of the melting line, the dashed line shows metastable extensions of the melting line, *FE* the crystal spinodal, K_2 the melting line endpoint. The sign × signifies starting states in studying nucleation.

This article is copyrighted as indicated in the article. Reuse of AIP content is subject to the terms at: http://scitation.aip.org/termsconditions. Downloaded to IP: 35.8.11.3 On: Fri, 29 Jan 2016 23:26:19

$$c_{ij} = \left\langle c_{ij}^{B} \right\rangle + \left\langle c_{ij}^{F} \right\rangle + \left\langle c_{ij}^{K} \right\rangle . \quad (17)$$

Here, the first, second, and third terms in the right-hand side of Eq. (17) present the Born (static), fluctuation, and kinetic (thermal) contributions, respectively. The angle brackets signify the ensemble average.

The elastic constants calculated by Eq. (17) determine the behavior of an unloaded crystal ($p = 0$). In a loaded state, these constants do not take into account the work that must be done against an external load by the forces caused by an additional small deformation.[33] At a given hydrostatic pressure p, for the shear moduli of a cubic crystal, we have $\tilde{c}_{44} = c_{44} - p$, $\tilde{c}'_{44} = (c_{11} - c_{12})/2 - p$.

For an anisotropic solid, $\tilde{c}_{44}/\tilde{c}'_{44} > 0$. With respect to shear stresses, a crystal of cubic symmetry will be equivalent to an isotropic solid whose shear modulus μ_s is the orientation-averaged value of the moduli $\tilde{c}_{44}$ and $\tilde{c}'_{44}$, i.e., $\mu_s = (3\tilde{c}_{44} + 2\tilde{c}'_{44})/5$.[34] Fig. 3 shows the density dependence of moduli K_s, $\tilde{c}_{44}$, $\tilde{c}'_{44}$, and μ_s in the range of state parameters investigated at two values of temperature.

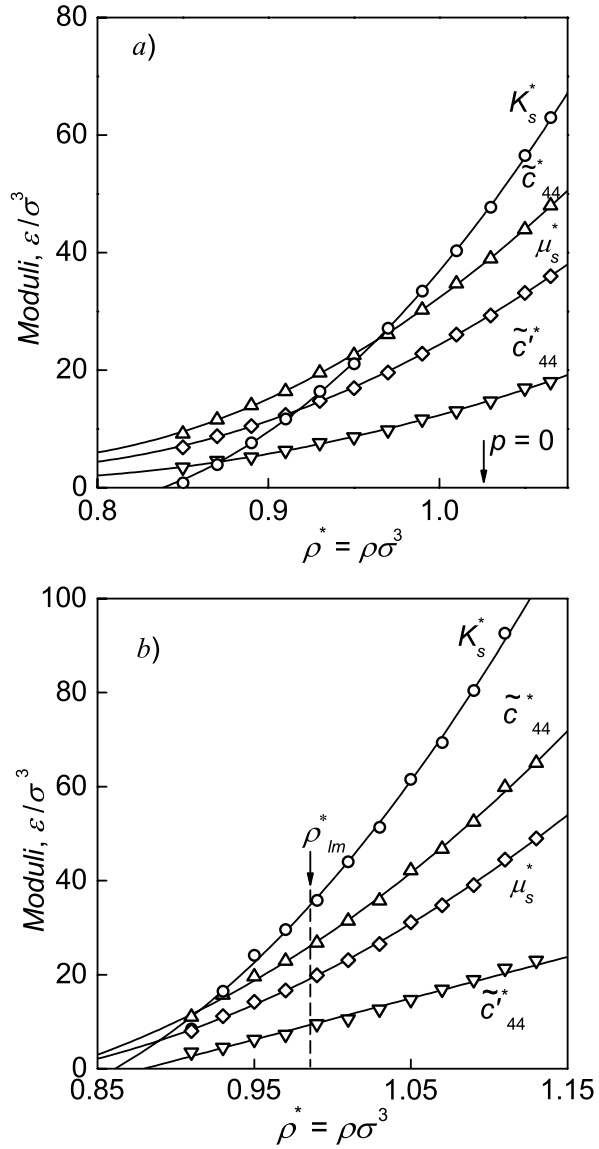

FIG. 3. Density dependence of the bulk modulus of elasticity K_s (○), shear moduli of elasticity $\tilde{c}_{44}$ (△), $\tilde{c}'_{44}$ (▽), and the orientation-averaged shear modulus μ_s (◇) at temperatures (a) $T^* = 0.4$ and (b) $T^* = 0.85$. The densities corresponding to pressure $p = 0$ and the melting line ρ_{lm} are indicated.

C. Central symmetry parameter and identification of liquid droplets and voids in a crystal

In investigations of the process of rupture of a crystal, structure use was made of the CSP, which for every particle in a fcc crystal was calculated by the following formula:[35]

$$\psi_j = \sum_{i=1,6} \left| \vec{r}_{j,i} + \vec{r}_{j,i+6} \right|^2 . \quad (18)$$

Here, $\vec{r}_{j,i}$ and $\vec{r}_{j,i+6}$ are radius vectors drawn from the particle j to two neighboring particles. The summation in Eq. (18) is made over pairs of oppositely directed vectors for six nearest pairs of particles with the smallest value of $\left| \vec{r}_{j,i} + \vec{r}_{j,i+6} \right|^2$. When the particles are fixed at the sites of an ideal fcc lattice, $\psi_j = 0$.

In the MD simulations, the values of ψ_j were calculated every 1000 time steps. In homogeneous states of the crystal phase, the value of $\psi_j^* = \psi_j/\sigma^2$ was not larger than 3 (Fig. 4(a)). When a void forms in a crystal for some particles, ψ_j^* reaches values that are an order of magnitude larger than 3 (Fig. 4(b)). Visualization of this process has shown that all the particles with $\psi_j^* > 3$ become localized at the void surface.

No considerable increase in the value of ψ_j was observed during the formation of liquid-phase inclusions in a crystal. In this case, to isolate particles that belonged to the new phase, the value of the CSP $\overline{\psi}_j$ average over five values of ψ_j (on 5000 time steps) was calculated. The averaged values of CSP particles located at the sites of the crystal lattice are approximately two times lower than those of the particles which have left the sites. This procedure allowed separating liquid-like particles from crystal-like ones. The value of $\overline{\psi}_j^*$ equal to 1.5 was taken as the boundary of their separation (Fig. 4(c)).

IV. RESULTS AND DISCUSSIONS

A. Melting mechanism at limiting crystal superheating

For investigating the process of nucleation of a new phase close to the boundary of limiting stretching of a LJ crystal, use was made of the following procedure. The starting (weakly metastable) state was chosen on every isotherm, from which the crystal was transferred into a region where the nucleation of new-phase inclusions had time to take place during the simulation. The starting states are marked in Fig. 2 by crosses. In a starting state, the system under investigation was brought to equilibrium within no less than 10^5 time steps. Then, within 10^3 time steps, by means of stretching in all directions, it was brought to the initial state. After the transition, the temperature was corrected (10^3 time steps) and the system relaxed freely to the state of local equilibrium. After relaxation, the crystal phase was in a homogeneous metastable state for no less than 3×10^5 time steps, whereupon a new-phase nucleus was formed in it. The choice of the initial homogeneous state was determined by the time of existence of a metastable crystal phase in it, which in its turn depended on the number of particles in the system. The points at the ends of the isotherms presented in Fig. 2 refer to systems with different numbers of

This article is copyrighted as indicated in the article. Reuse of AIP content is subject to the terms at: http://scitation.aip.org/termsconditions. Downloaded to IP: 35.8.11.3 On: Fri, 29 Jan 2016 23:26:19

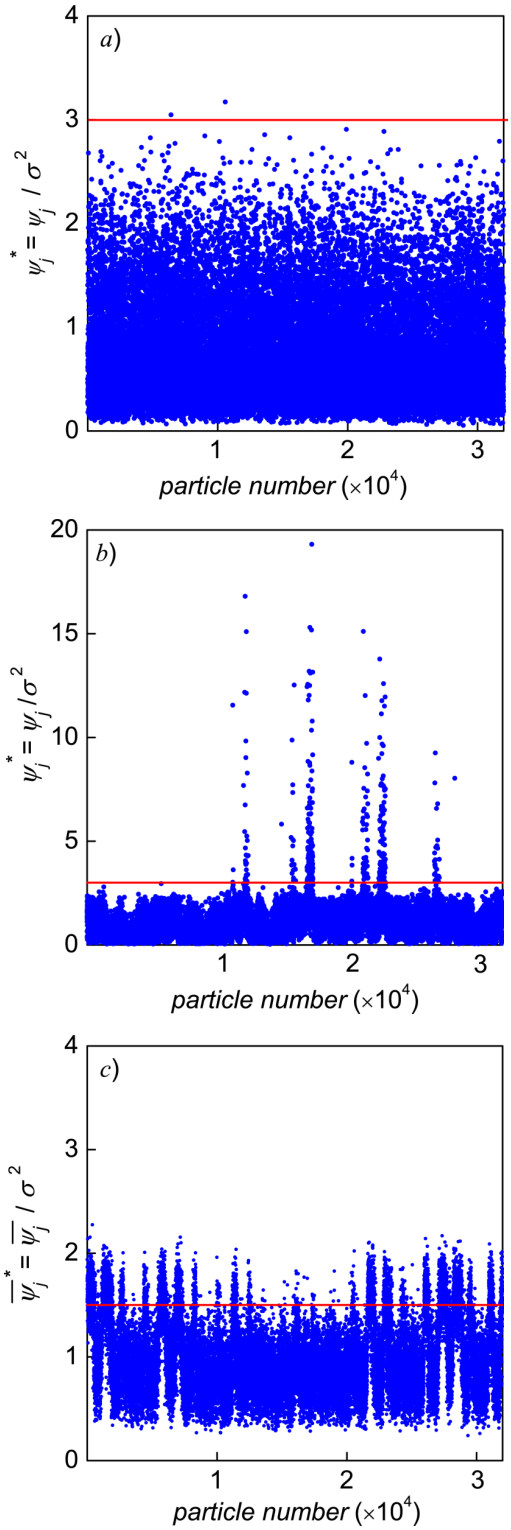

FIG. 4. Central symmetry parameter of (a) a homogeneous crystal phase ($T^* = 0.4$, $\rho^* = 0.84$), (b) a crystal phase with a void ($T^* = 0.4$, $\rho^* = 0.84$), and (c) a crystal phase with a liquid droplet ($T^* = 0.85$, $\rho^* = 0.91$) in a system $N = 32\,000$. The horizontal line separates particles at the sites of the crystal lattice from those that have left the sites.

particles. The endpoint on each isotherm has been obtained at $N = 32\,000$.

At temperatures $T^* = 0.7$ and 0.85, which are higher than the temperature of the endpoint of the melting line, a rupture of a crystal structure was accompanied by an abrupt decrease in the temperature and a synchronous growth of the global CSP Ψ (Fig. 5(a)). The value of the CSP, $\Psi = \sum_j \psi_j / N$, averaged over all the particles of the system was taken as the global CSP.

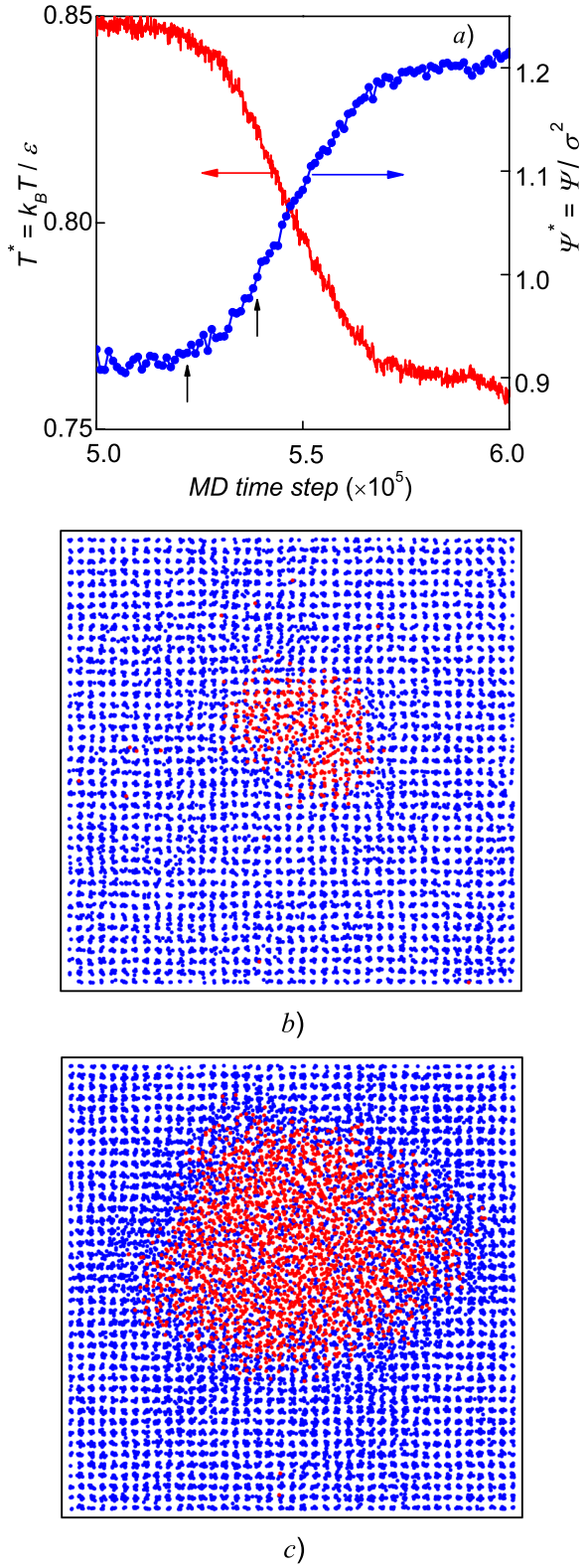

FIG. 5. (a) Evolution of the global CSP and temperature with the appearance of liquid-phase inclusions in a crystal ($T^* = 0.85$, $\rho^* = 0.91$, $N = 32\,000$). A two-dimensional projection of the particle configuration in the system (a layer 4.5σ thick is isolated) after (b) 52×10^4 and (c) 54×10^4 time steps, which are shown with vertical arrows in a figure (a).

This article is copyrighted as indicated in the article. Reuse of AIP content is subject to the terms at: http://scitation.aip.org/termsconditions. Downloaded to IP: 35.8.11.3 On: Fri, 29 Jan 2016 23:26:19

Figure 5(b) shows a cell cut after 52×10^4 time steps, when the global CSP registers the beginning of a phase transition. The forming nucleus has a near-spherical shape and is a liquid-phase nucleus. The subsequent growth of the nucleus over the course of 2×10^4 steps did not change its shape (Fig. 5(c)). Then, the nucleus was elongated in one of the planes parallel to the cell faces, and in the central part of the cell there formed a liquid-phase layer surrounded on two sides by the crystal phase. This configuration retained its stability in the process of the subsequent system evolution.

A different pattern of phase decay was observed at a temperature $T^* = 0.4$. Here, as is seen from Fig. 6(a), the beginning of a phase transition is accompanied by an increase in both the global CSP and temperature. The rupture of a crystal structure began with the formation of a void (Fig. 6(b)). The void is free from particles, and the particles at its boundary have a considerable mobility. The rate of the void growth is approximately 10 times higher than that of the droplet growth. The growth of a void (Fig. 6(c)) was accompanied by considerable shifts of crystal-phase particles from the lattice sites. The void shape is close to spherical and does not change throughout the whole simulation. After the system went into equilibrium, the crystal order was reconstructed in the phase that surrounded the void, and the configuration "crystal with a void" was retained throughout the subsequent 10^6 simulation time steps.

The system evolution at a temperature $T^* = 0.55$ is illustrated in Fig. 7(a). The monotonic growth of the global CSP is accompanied by a temperature lowering at the beginning of phase decay, which is subsequently replaced by its abrupt increase. The temperature lowering, as has been mentioned above, is characteristic of the nucleation of a liquid phase, whereas its increase is observed during the formation of a void. It should also be mentioned that on the whole time interval within which the temperature was falling, the values of ψ_j^* were smaller than 3. The beginning of a temperature increase was accompanied by a two- or three-fold increase of the CSP for some particles of the system. The configurations of particles in a cell presented in Figs. 7(b) and 7(c) point to the fact that in a crystal, initially there forms a liquid phase, and then a void forms inside it.

Thus, a transition from high to low temperatures is accompanied by a qualitative change in the nucleation process. If the nucleation of a liquid phase is characteristic of high temperatures, at low temperatures, the disintegration of a crystal structure begins with the formation of a void. The region of the change of nucleation regimes falls on a temperature close to that of the endpoint of the melting line ($T_{K2}{}^* = 0.529$).

Let us now analyze the nucleation processes observed from the viewpoint of thermodynamics. Let us assume that in a stretched crystal at a positive or a small negative pressure p, there forms a critical liquid-phase nucleus. At equilibrium between the nucleus and its surroundings, the equality of the chemical potentials that refer to the nucleus and the crystal $\mu_l(p_*, T) = \mu_{cr}(p_s, T)$ must hold true. Here, p_* is the pressure inside a critical liquid nucleus. The pressure p_* is lower than the pressure on a phase equilibrium line p_m. The value of $p_m - p_*$ increases with the increase in the stretching $p_m - p_s$ of the crystal phase. We shall make some evaluations of the respective

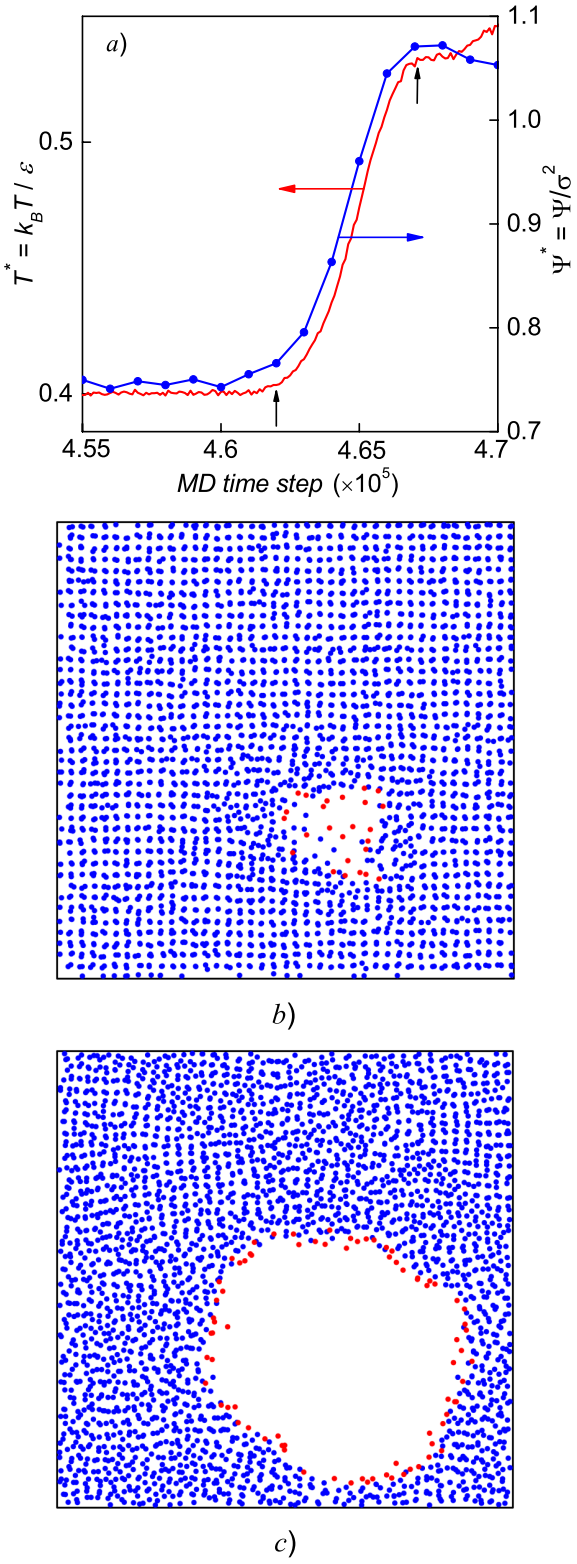

FIG. 6. (a) Evolution of the global CSP and temperature with the appearance of a void ($T^* = 0.4$, $\rho^* = 0.84$, $N = 32\,000$). A two-dimensional projection of the particle configuration in the system (a layer 4.5σ thick is isolated) after (b) 462×10^3 and (c) 467×10^3 time steps, which are shown with vertical arrows in a figure (a).

quantities making use of the equations of liquid and crystal states from Ref. 20.

At a temperature $T^* = 0.85$ and a pressure in the crystal phase $p_s^* = 0.178$, which corresponds to a stretching $p_m^* - p_s^*$

This article is copyrighted as indicated in the article. Reuse of AIP content is subject to the terms at: http://scitation.aip.org/termsconditions. Downloaded to IP: 35.8.11.3 On: Fri, 29 Jan 2016 23:26:19

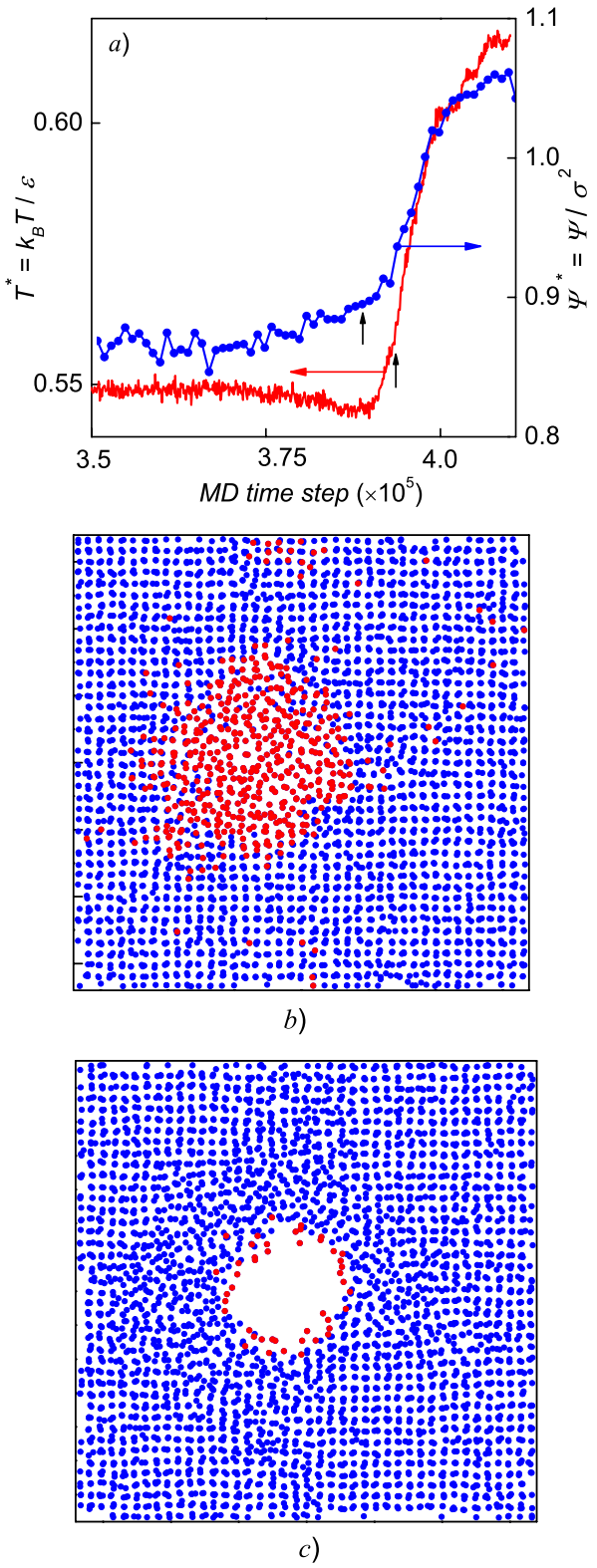

FIG. 7. (a) Evolution of the global CSP and temperature with the appearance of a new-phase inclusion ($T^* = 0.55$, $\rho^* = 0.86$, $N = 32\,000$). A two-dimensional projection of the particle configuration in the system (a layer 4.5σ thick is isolated) after (b) 388×10^3 and (c) 393×10^3 time steps, which are shown with vertical arrows in a figure (a).

= 1.773, the reduced pressure in a critical nucleus is approximately 0.35, which is 2.7 times higher than the pressure at the liquid–gas critical point and ensures a stable state of the liquid phase in a critical nucleus. Similar calculations for $T^* = 0.7$ and $p_s^* = -1.255$ (the endpoint on the isotherm, Fig. 2) testify that the pressure in a critical nucleus exceeds the pressure on the spinodal of a stretched liquid only slightly ($p_{sp}^* \approx -1.0$). Thus, in a critical nucleus, the liquid is in a metastable (stretched) state.

At a temperature $T^* = 0.55$ and a pressure lower than p_m, no equilibrium (stable or metastable) liquid phase with a chemical potential equal to the crystal chemical potential $\mu_{cr}(p_s, T)$ may be put in correspondence with the crystal phase because such a liquid can exist neither in a stable nor a metastable state. The formation of a liquid phase at $T^* = 0.55$ observed at the initial stage of phase decay is most likely connected with the nonequilibrium character of the initial stage of the nucleation process.

Thus, at $T < T_{K2}$, liquid-phase nuclei cannot form. Here, not only the liquid phase in a nucleus is labile but also the crystal–liquid interfacial free energy is not determined either.[36] As a result, the phase decay of a crystal proceeds by way of nucleation and growth of voids.

B. Kinetic aspects of nucleation of a new phase

At nucleation simulation, one should differentiate several characteristic times. The first characteristic time t_1 is the time of the crystal transfer from a stable or a slightly metastable state to the metastable (initial) state under investigation. It is assumed that on the interval t_1, nuclei do not arise owing to the smallness of this interval. After a homogeneous system is brought to the prescribed values of p and T, an equilibrium is established in it in the time t_{rel}. The time t_{rel} is determined by the slowest of the relaxation processes (thermal conductivity, restructuring, etc.). The next characteristic time is the expectation time for the appearance of a viable nucleus τ in a metastable system. Since a spontaneous formation of a nucleus is a random event, only the mean expectation time for a nucleus $\bar{\tau}$ has a certain physical meaning. The value of $\bar{\tau}$ is inversely proportional to the number of particles in the system (the system volume) and depends on the degree of metastability. For the nucleation of a new phase to proceed from a state of local equilibrium with fixed values of p and T, the condition $\bar{\tau} >> t_{rel}$ must be fulfilled. The value of $\bar{\tau}$ does not depend on the zero time in view of the Poisson law of distribution of expectation times for the nucleus appearance τ.[12] If we designate by J the average number of viable nuclei that appear in a unit time in a unit volume, in a stationary case, we have $JV = \bar{\tau}^{-1}$. By the results of nucleation simulation in a stretched crystal, from this relation, one can evaluate J for states of limiting stretching. At $N = 32\,000$ and $\rho^* = 0.85$–0.9, we have $V^* = 37\,650$ - $35\,550$. The characteristic expectation time for the nucleus appearance (see Section IV A) identified with the time $\bar{\tau}$ is approximately $(3\text{–}5) \times 10^5$ time steps or 700–1160 reduced units. Thus, $J^* = (2\text{–}4) \times 10^{-8}$.

The value of J may be calculated in the framework of classical nucleation theory,[37] which relates the nucleation rate to the work of formation of a critical nucleus,

$$J = \rho_s B \exp(-W_*/k_B T) = J_0 \exp(-W_*/k_B T), \qquad (19)$$

where B is the kinetic factor that characterizes the average rate of passage of nuclei through the critical size, and ρ_s is the crystal phase density.

This article is copyrighted as indicated in the article. Reuse of AIP content is subject to the terms at: http://scitation.aip.org/termsconditions. Downloaded to IP: 35.8.11.3 On: Fri, 29 Jan 2016 23:26:19

To evaluate the kinetic factor at the formation of a liquid droplet in a superheated crystal, we shall use the results of crystallization theory, in which the value of B is determined by the rate of elementary acts of attachment of particles to the nucleus surface and their departure from the nucleus surface into the crystal.[38] By the data of Ref. 39, the kinetic factor depends only slightly on the degree of metastability of the initial phase, and in the order of magnitude $B = 10^{10}$–10^{11} s^{-1}, or in reduced units $B^* = 10^{-2}$–10^{-1}. Using this value of B and data on the nucleation rate, one can evaluate the work of formation of a critical nucleus from Eq. (19). In our simulation, $W_*/k_BT \approx 10$–20.

If the phase decay of a superheating crystal proceeds through the formation and growth of voids, the factor retarding their growth will be the energy dissipation (viscosity η). An allowance for the viscosity in equations of motion of solids may be realized in the same way as in the case of liquids.[40] Then, using the solution of the problem on cavitation in a non-volatile liquid,[37,41] we have

$$B = \frac{\rho_s R_*}{2\eta}(k_BT\gamma_{sv})^{1/2}. \tag{20}$$

Equation (20) makes it possible to evaluate the order of magnitude of the kinetic factor in Eq. (19). If the viscosity of a crystal is taken equal to that of a superheated liquid at the same value of density ($\rho_s^* = 0.85$), then $\eta^* \approx 6.2$,[42] the radius of a critical nucleus $R_*^* \approx 2.0$ (see Fig. 6(b)), and the LJ crystal–gas interfacial free energy $\gamma_{sv}^* \approx 1.82$.[43] Using these values, we have $B^* \approx 5 \cdot 10^{-2}$, and $J_0^* \approx 4 \cdot 10^{-2}$, which practically coincides with the value of J_0 for nucleation of a liquid droplet. The latter signifies an approximate constancy of the reduced nucleation work on the whole line of limiting stretching at temperatures both higher and lower than the endpoint of the melting line.

C. Work of formation of a critical nucleus

Figure 8 presents a p, T–projection of the phase diagram of a LJ system in a region adjoining the triple point. At the scale of the figure, at temperatures close to and lower than the temperature of the endpoint of the melting line, the stretching achieved in the simulation coincides with the spinodal ones. Here, the disintegration of a crystal phase proceeds by way of nucleation and growth of voids. At $T > T_{K2}$, nuclei are liquid droplets, and the limiting stretching of a crystal phase achieved in simulation is lower than the spinodal ones. The disagreement between the kinetic and thermodynamic stability boundaries increases with increasing temperature.

The results of MD simulation and the equations obtained in Section II will be used to estimate the work of formation and some other parameters of critical nuclei in a superheated (stretched) crystal. As is evident from Eq. (5), the presence of elastic energy e makes impossible the formation of spherical liquid-phase nuclei at small crystal superheatings. The boundary of an elastic thermodynamic hysteresis is shown in Fig. 8 as a dashed-dotted line. In calculations, use was made of the data on the crystal–liquid interfacial free energy from Ref. 36. The bulk moduli of the liquid and the crystal phase were calculated by the equations of state of Refs. 20 and 30. Data on the parameters of the melting line[17,20] were used in determining

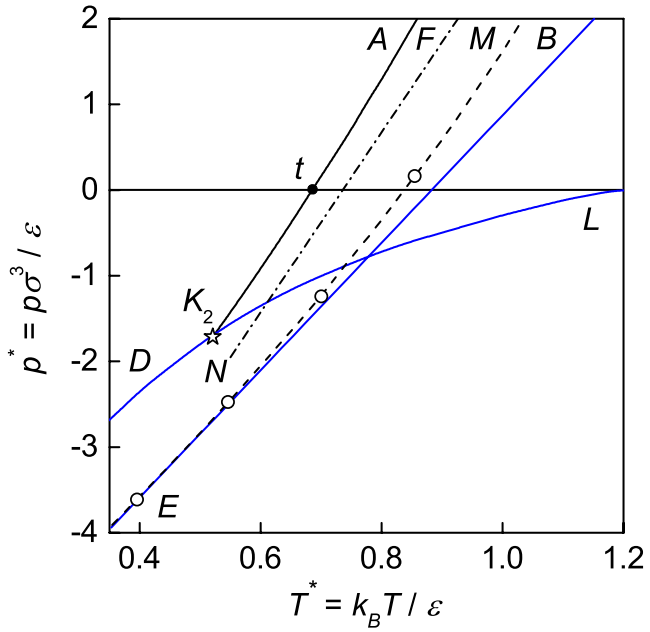

FIG. 8. P, T–projection of the phase diagram of a LJ system. AtK_2 is the melting line, DK_2L the spinodal of a stretched liquid, BE the spinodal of a superheated crystal, ME the line of the limiting stretching of crystal phase, FN the boundary of elastic thermodynamic hysteresis, t the triple point, and K_2 the melting line endpoint.

the specific thermodynamic potentials of the coexisting phases and their difference, Δg (Eq. (6)).

The results of calculating the reduced work of formation of a critical-sized liquid droplet W_*/k_BT at a temperature $T^* = 0.85$ are presented in Fig. 9. Eqs. (5) and (12) give qualitatively different behaviors of W_* not only close to the melting line but also close to the spinodal. If at the approach to the boundary, where $K_s = 0$, the shear modulus μ_s does not become equal to zero, then at this boundary (provided that

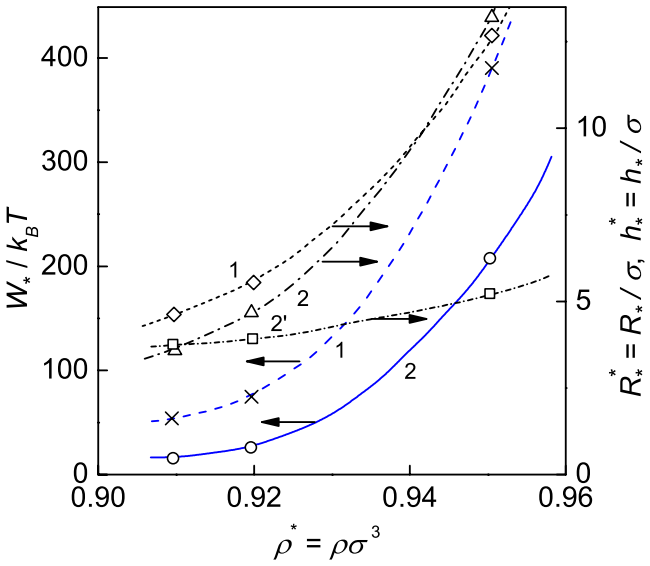

FIG. 9. Reduced work of formation and characteristic dimensions of a critical liquid droplet in the form of a sphere (1) and a lense (2). The dashed line (2) shows the lense radius, the dashed-dotted line (2′) the lense height. Calculations by Eqs. (5), (12) and (4), (10), (11).

This article is copyrighted as indicated in the article. Reuse of AIP content is subject to the terms at: http://scitation.aip.org/termsconditions. Downloaded to IP: 35.8.11.3 On: Fri, 29 Jan 2016 23:26:19

$\gamma_{sl} \neq 0$), the work of formation of a critical nucleus, according to Eq. (12), has a finite value.

As is evident from Fig. 9, close to the boundary of the limiting stretching, the work of formation of a liquid-phase nucleus calculated by Eq. (5) (spherical droplet) is approximately 3 times as large as that calculated by Eq. (12) (lense). In going deeper into a metastable region, both the radius and the height of a lense-shaped nucleus decrease, with the nucleus radius decreasing much more appreciably than the height, and close to the boundary of the limiting stretching these two parameters take similar values. Viable nuclei that form close to the boundary of the limiting stretching will have a shape which is only slightly different from a spherical one. According to Eqs. (10) and (12), at $T^* = 0.85$ and $\rho^* = 0.91$, the effective radius of a critical nucleus $R_*^* \approx 3.5$, and $W_*/k_BT \approx 15$. These values are in good agreement with the results of simulation (Fig. 5(b)) and evaluations of the reduced work of formation of a critical nucleus by classical nucleation theory (Eq. (19)).

At temperatures below T_{K2}, a phase decay begins with the formation of a void, which, as is seen from Figs. 6(b) and 6(c), has a shape close to spherical. The critical radius of a lense-shaped void at the limiting-stretching boundary at $T^* = 0.4$ and $\rho^* = 0.845$, according to Eq. (14), is $R_*^* = 1.56$. The limiting stretching of a crystal phase $\Delta p_n^* = 3.615$ coincides here with the stretching corresponding to the crystal spinodal Δp_{sp}, on which $K_s = 0$ and $\upsilon_s = -1$. If we equate the volumes of a critical lense-shaped void and a certain spherical void of radius R_{eff}, then from Eqs. (14) and (15) at $\upsilon_s = -1$, we will have $(R_{eff}/R_*)^3 = 2\Delta p_n/\pi\mu_s$. From this, it follows that the value of R_{eff}/R_* equals 0.82, i.e., at the limiting-stretching boundary, a void ($T < T_{K2}$), as well as a liquid droplet ($T > T_{K2}$), must have a near-spherical shape. As Δp_n decreases and the line of crystal–gas phase equilibrium is approached, the value of R_{eff}/R_* tends to zero ($\upsilon_s \leq 0.5$, $\mu_s \geq 0$).

For the conditions indicated above, the work of formation of a critical-sized void is $W_*/k_BT \approx 22$. This value is also close to the estimation of the value of W_* from classical nucleation theory by data on the mean expectation time for a critical nucleus. Thus, from molecular dynamics simulation, it follows that in a crystal phase at $T < T_{K2}$ it is possible to achieve breaking stresses that practically coincide with the spinodal ones. According to Eqs. (14)–(16), the final value of W_* on the spinodal is a result of the independence of γ_{sv} from the radius of curvature of the crystal–gas interface. If at $p \to p_{sp}$ the value of $\gamma_{sv} \to 0$, then $W_* = 0$, and the spinodal will be unattainable in molecular dynamics simulation.

From the van der Waals gradient theory[44] and the method of the density functional[45] for fluid phases, it follows that on the spinodal W_* becomes zero. At the same time, there is a different point of view, which assumes the existence of an energy barrier on the spinodal.[46] Gibbs[47] in discussing the question of comparison of the stability boundary in reference to continuous phase changes (spinodal), with the stability boundary in reference to the process of formation of new-phase nuclei, pointed out that these boundaries must be close to each other.

If nucleation in a superheated crystal proceeds at temperatures above T_{K2}, the line of the limiting stretching (superheating) departs from the spinodal line (see Fig. 9). In a LJ system at the triple point temperature, the interfacial free energy at a crystal–liquid interface is approximately three times smaller than that at a crystal–gas interface; therefore, the formation of a liquid-phase nucleus is connected with much smaller expenditures of energy than in the case of a gas-phase nucleus. Spontaneous melting of a crystal phase at a considerable distance from the spinodal may be connected with the decrease in the crystal instability in reference to the shear deformation. At positive pressures, the condition $\tilde{c}'_{44} = 0$ is achieved before K_s becomes zero (see Fig. 3(b)).

V. CONCLUSIONS

A phase decay of a crystal state may proceed through melting, with the formation of a liquid phase, or by way of creating a discontinuity, with the formation of cracks and voids, and a subsequent fracture of a solid. Which of the indicated processes will be determining depends on many factors: the thermodynamic state of the crystal, the character of the process being conducted, the mechanism of nucleation of a new phase, etc. An isothermal decrease in the pressure in a crystal phase below the pressure of crystal–liquid coexistence at temperatures higher than that of the endpoint of the sublimation line K_1 (see Fig. 1, arrow *a*) may lead only to the formation of a liquid phase. The same result will be observed under an isobaric heating of a crystal at a pressure higher than that of the point K_1. When the temperature and the pressure in the crystal are lower than the temperature and the pressure of the endpoint K_1, respectively, at an intersection of the melting and sublimation lines, the nucleation of both a liquid and the gas phase is possible. In particular, being stretched along the arrow *b* in Fig. 1, a crystal phase initially crosses the sublimation line, and the crystal becomes unstable against the formation of a nucleus of a gas phase in it, but nothing forbids the formation of a nucleus of a metastable liquid phase in the crystal as well. The answer to the question a nucleus of which of the phases — liquid or gas — will be the first to appear is well known.[48] The first will be the phase characterized by a higher nucleation rate. Since the nucleation rate is mainly determined by the work of nucleus formation, the phase formed will possess a smaller activation energy. Such a competition between incipient phases is observed, for example, in supercooled liquids at negative pressures, where crystal-phase nuclei and voids are formed.[49]

A considerable contribution to the work of formation of a critical nucleus is made by the interfacial free energy. Owing to the smaller value of the free energy of a liquid–solid interface as compared to a solid–gas interface, at a high degree of metastability, the nucleation of a liquid-phase nucleus inside a solid proceeds much more easily than of a bubble.

We have used the method of molecular dynamics simulation to investigate the process of formation of a new phase in a Lennard-Jones fcc crystal at temperatures above and below that of the endpoint of the melting line. Nucleation proceeded in conditions of constancy of the number of particles, volume, and total energy. The phase decay dynamics was registered by changes in the parameter of central symmetry and the temperature in the system. At temperatures $T > T_{K2}$, a phase decay in the crystal began with the appearance of a liquid-phase nucleus. The formation of a nucleus leads to a decrease in

This article is copyrighted as indicated in the article. Reuse of AIP content is subject to the terms at: http://scitation.aip.org/termsconditions. Downloaded to IP: 35.8.11.3 On: Fri, 29 Jan 2016 23:26:19

the potential energy in the solid phase and its increase in the liquid one, with the second factor exceeding quantitatively the first one, which causes a decrease in the kinetic energy and temperature of the system. A crystal–liquid phase transition ended with the formation of a flat interface in the cell.

At $T < T_{K2}$, the homogeneity of a crystal phase was disturbed in the process of nucleation and growth of voids. The appearance of a void was accompanied by an increase in the temperature. The latter was connected with the decrease in the potential energy of a crystal phase as a result of tensile stress relieving. In the transition region at temperatures close to T_{K2}, a phase decay proceeded through the formation of an intermediate liquid phase and its cavitation discontinuity.

We have interpreted the results obtained in the framework of classical nucleation theory. It is shown that in the thermodynamics of nucleation the determining role is played by the elastic stresses that arise owing to the difference in the phase density. At the same time, the elastic forces do not practically affect the nucleation dynamics, which is determined by the macroscopic processes at the interface.

The magnitude of the work of formation of a critical nucleus depends considerably on its shape. With elastic stresses, the spherical shape of a nucleus is not, generally speaking, optimum even in an isotropic solid medium. At small superheatings (stretching) of a solid phase, the nucleus must be highly flattened in one dimension and have a disk-shaped (lense-shaped) form.

With an increase in superheating (stretching), close to the boundary of limiting superheating, lense-shaped nuclei stake a spherical form. This conclusion of a thermodynamic consideration of the nucleation process in a crystal is confirmed by data of MD simulation.

At temperatures below that of the endpoint K_2 and nucleation rates characteristic of molecular dynamics simulation voids, too, have a shape close to spherical. The large value of the crystal–gas interfacial free energy together with elastic deformations leads to a qualitatively different result, which is not characteristic, for instance, of liquid–gas or crystal–liquid phase transitions (at $T > T_{K2}$): the kinetic stability boundary (the limiting stretching line) of the crystal phase practically coincides with the thermodynamic stability boundary (spinodal). At $T > T_{K2}$, with an increase in the temperature, these stability boundaries diverge.

In conclusion, we mention that in investigating spontaneous nucleation of inclusions in the form of liquid droplets and voids in a metastable crystal, we were not interested in the mechanisms of their formation in a subcritical stage. The discussion of these problems can be found in Refs. 50 and 51. The interpretation of the results of molecular dynamics simulation is based on the relations of the linear theory of elasticity. Visualization of the nucleation process (Figs. 5-7) testifies that at the initial stage of formation and growth of a void a zone of elastoplastic deformation forms around it. The effect of a plastic interlayer on the work of formation of a liquid-phase nucleus in a superheated crystal was theoretically considered in Ref. 21.

ACKNOWLEDGMENTS

The work has been performed with a financial support of the Russian Scientific Foundation (Project No. 14-19-00567).

[1]L. D. Landau and E. M. Lifshitz, *Statistical Physics Part 1*, 3rd ed. (Pergamon Press, Oxford, 1980).
[2]S. E. Khaikin and N. R. Bene, C. R. Acad. Sci. URSS **23**, 31 (1939).
[3]L. Grabaek, J. Bohr, H. N. Andersen *et al.*, Phys. Rev. B **45**, 2628 (1992).
[4]J. W. Herman and H. E. Elsayed-Ali, Phys. Rev. Lett. **69**, 1228 (1992).
[5]G. I. Kanel, V. E. Fortov, and S. V. Razorenov, Uspekhi Fiz. Nauk **177**, 809 (2007); Phys.-Usp. **50**, 771 (2007).
[6]Z. Zhang, Z. H. Jin, L. H. Zhang, M. L. Sui, and K. Lu, Phys. Rev. Lett. **85**, 1484 (2000).
[7]D. S. Ivanov and L. V. Zhigibei, Phys. Rev. B **68**, 064114 (2003).
[8]M. Born, J. Chem. Phys. **7**, 591 (1939).
[9]F. A. Lindeman, Phys. Z. **11**, 609 (1910).
[10]H. J. Fecht and W. L. Johnson, Nature **334**, 50 (1988).
[11]J. L. Tallon, Nature **342**, 658 (1989).
[12]V. P. Skripov, *Metastable Liquids* (Wiley, New York, 1974).
[13]K. Lu and Y. Li, Phys. Rev. Lett. **80**, 4474 (1998).
[14]Z. H. Jin, P. Gumbsch, K. Lu, and E. Ma, Phys. Rev. Lett. **87**, 055703 (2001).
[15]G. E. Norman and V. V. Stegailov, Dokl. Phys. **47**, 667 (2002).
[16]S.-N. Luo, T. J. Ahres, T. Cağin *et al.*, Phys. Rev. B **68**, 134206 (2003).
[17]V. G. Baidakov and S. P. Protsenko, Phys. Rev. Lett. **95**, 015701 (2005).
[18]X.-M. Bai and M. Li, Phys. Rev. B **72**, 052108 (2005).
[19]A. Yu. Kuksin and A. V. Yanilkin, Dokl. Akad. Nauk **413**, 615 (2007).
[20]V. G. Baidakov and S. P. Protsenko, J. Exp. Theor. Phys. **103**, 876 (2006).
[21]I. M. Lifshitz and L. S. Gulida, Dokl. Akad. Nauk SSSR **87**, 377 (1952).
[22]A. L. Roitburd, Sov. Phys. Solid State **25**, 33 (1983).
[23]V. I. Motorin, Sov. Phys. Solid State **29**, 732 (1987).
[24]E. A. Brener, S. V. Iordanskii, and V. I. Marchenko, Phys. Rev. Lett. **82**, 1506 (1999).
[25]V. I. Motorin and S. L. Musher, J. Chem. Phys. **81**, 465 (1984).
[26]A. A. Griffith, Philos. Trans. R. Soc., A **221**, 163 (1920).
[27]I. N. Sneddon, Proc. R. Soc. A **187**, 229 (1946).
[28]S. Plimpton, J. Comput. Phys. **117**, 1 (1995).
[29]H. J. C. Berendsen, J. P. M. Postma, W. F. van Gunsteren, A. DiNola, and J. R. Haak, J. Chem. Phys. **81**, 3684 (1984).
[30]V. G. Baidakov and S. P. Protsenko, Dokl. Akad. Nauk **402**, 754 (2005).
[31]J. H. Wang, J. Li, S. Yip, D. Wolf, and S. Phillpot, Physica A **240**, 396 (1997).
[32]T. Cağin and R. J. Ray, Phys. Rev. B **38**, 7940 (1988).
[33]J. Wang, J. Li, S. Yip, S. Phillpot, and D. Wolf, Phys. Rev. B **52**, 12627 (1995).
[34]S. Hess and M. Krögen, Phys. Rev. E **64**, 011201 (2001).
[35]C. L. Kelchner, S. J. Plimpton, and J. C. Hamilton, Phys. Rev. B **58**, 11085 (1998).
[36]V. G. Baidakov, S. P. Protsenko, and A. O. Tipeev, J. Chem. Phys. **139**, 224703 (2013).
[37]Ya. B. Zeldovich, J. Exp. Theor. Phys. **12**, 525 (1942).
[38]D. Turnbull and J. C. Fisher, J. Chem. Phys. **17**, 71 (1949).
[39]V. G. Baidakov and A. O. Tipeev, J. Chem. Phys. **136**, 174510 (2012).
[40]L. D. Landau and E. M. Lifshitz, *Theory of Elasticity* (Pergamon Press, Oxford, 1970).
[41]A. V. Prokhorov, Dokl. Akad. Nauk SSSR **239**, 1323 (1978).
[42]V. G. Baidakov, S. P. Protsenko, and Z. R. Kozlova, J. Chem. Phys. **137**, 164507 (2012).
[43]J. Q. Broughton and G. H. Gilmer, J. Chem. Phys. **84**, 5741 (1986).
[44]J. W. Cahn and J. E. Hilliard, J. Chem. Phys. **31**, 688 (1959).
[45]T. V. Bykov and X. C. Zeng, J. Chem. Phys. **125**, 144515 (2006).
[46]J. H. Hollomon and D. Turnbull, Prog. Met. Phys. **4**, 333 (1953).
[47]J. W. Gibbs, *The Collected Works Volume 2. Thermodynamics* (Longmans and Green, New York, 1928).
[48]M. Volmer, *Kinetik der Phasenbilding* (Steinkopff, Drezden, Leipzig, 1939).
[49]V. G. Baidakov, K. S. Bobrov, and A. S. Teterin, J. Chem. Phys. **135**, 054512 (2011).
[50]X. M. Bai and M. Li, Phys. Rev. B **77**, 134109 (2008).
[51]G. E. Norman and A. V. Yanilkin, Phys. Solid State **53**, 1614 (2011).

This article is copyrighted as indicated in the article. Reuse of AIP content is subject to the terms at: http://scitation.aip.org/termsconditions. Downloaded to IP: 35.8.11.3 On: Fri, 29 Jan 2016 23:26:19